Optica Applicata, Vol. XXXI, No. 4, 2001

Computer-assisted modified coupled-mode method for multiple-perturbed single-mode polarization-maintaining fibres

PAWEŁ WIERZBA

Technical University of Gdańsk, Faculty of Electronics, Telecommunication and Informatics, Department of Optoelectronics, ul. Narutowicza 11, 80–952 Gdańsk, Poland.

An extension to the modified coupled-mode method is presented, which allows the state of polarization to be calculated for a general case of a multiply perturbed fibre. Being based on numerical solution of coupled-mode equations, it can be used when an analytical solution of the coupled-mode equations does not exist, or is difficult to obtain. The present method was developed as a design tool for polarimetric optical fibre sensors. Short computation time was achieved as a result of modification to the solved coupled-mode equations.

1. Introduction

Modified coupled-mode method is a versatile tool for calculating the evolution of the state of polarization (SOP) along a single-mode fibre subjected to multiple perturbations, such as: transverse pressure, hydrostatic pressure, bending, Kerr effect, twist and Faraday effect. Since ellipticity of the fibre core and stress-induced birefringence can also be treated as perturbations, it is possible to apply this method to all types of single-mode polarization-maintaining (SMPM) fibres. A full account of the modified coupled-mode method can be found in papers [1] and [2]. Employing the theory presented therein, the SOP along the fibre can be expressed in an analytical form when perturbations acting upon the fibre are independent of the location z along it. In general case, however, an analytical description of the SOP does not exist.

The purpose of this paper is to devise a method by which the SOP in every location z along the section of a fibre can be calculated for an arbitrary SOP at the beginning of that section. Section 2 gives an outline of the modified coupled-mode theory needed to formulate, in Section 3, its computer-assisted extension. Finally, in Section 4, the method proposed is applied to the calculation of visibility in a twisted elliptical-core fibre subjected to pure bending.

2. Theory

The electric field vector $\mathbf{E}$ of electromagnetic field propagating in a single-mode fibre subjected to perturbations can be written as

$$\mathbf{E} = [A(z)e_x + B(z)e_y]\exp(j\omega t), \tag{1}$$

where: $A(z)$, $B(z)$ – complex amplitudes of electric field, e_x, e_y – distribution of electric field components in the fibre cross-section, ω – the angular frequency of electric field. Amplitudes $A(z)$ and $B(z)$ depend only on fibre axis coordinate z. They also have to satisfy coupled mode equation

$$\frac{\mathrm{d}}{\mathrm{d}z}\begin{bmatrix} A \\ B \end{bmatrix} = -j\begin{bmatrix} N_{11} & N_{12} \\ N_{12}^{*} & N_{22} \end{bmatrix}\begin{bmatrix} A \\ B \end{bmatrix} \tag{2}$$

where N_{ij} are coupling coefficients. Values of coupling coefficients depend upon perturbations acting on the fibre in the manner discussed in [1]. When coupling coefficients are independent of z (*i.e.*, $N_{ij} = \mathrm{const}(z)$), amplitudes $A(z)$ and $B(z)$ can be expressed as

$$\begin{bmatrix} A(z) \\ B(z) \end{bmatrix} = \begin{bmatrix} m_{11} & m_{12} \\ m_{21} & m_{22} \end{bmatrix}\begin{bmatrix} A_0 \\ B_0 \end{bmatrix}\exp\left(-j\frac{N_{11}+N_{22}}{2}z\right) \tag{3}$$

where A_0, B_0 – amplitudes $A(z)$ and $B(z)$ for $z = 0$ (*i.e.*, at the beginning of the analysed fibre section) and m_{ij} – mode coupling coefficients, given by:

$$m_{11} = \cos\left(\frac{\delta\beta}{2}z\right) - j\left(\frac{N_{11}-N_{22}}{\delta\beta}\right)\sin\left(\frac{\delta\beta}{2}z\right), \quad m_{22} = m_{11}^{*},$$

$$m_{21} = -j\left(\frac{2N_{21}}{\delta\beta}\right)\sin\left(\frac{\delta\beta}{2}z\right), \qquad m_{12} = -m_{21}^{*}, \tag{4}$$

with

$$\delta\beta = \sqrt{(N_{11}-N_{22})^2 + |2N_{12}|^2}. \tag{5}$$

When N_{ij} are functions of z (*i.e.*, $N_{ij} = N_{ij}(z)$), formulae (3)–(5) are no longer valid★. Even though amplitudes $A(z)$ and $B(z)$ can be calculated, by numerical solution of Eq. (2) for arbitrarily chosen A_0 and B_0, the process is time-consuming and it has to be repeated for every vector $[A_0, B_0]^T$ of interest.

★In some instances (*e.g.*, twisted elliptical core fibre) a coordinate system $\zeta\eta z$ exists, in which coupling coefficients N_{ij} do not depend on z. Solution of Eq. (2) can be found in this coordinate system using Eqs. (3)–(5) and subsequently expressed in terms of xyz coordinates. For full account of this method the reader is referred to Section 5 of [1]. However, it is impossible to apply this elegant method in a general case of a multiply perturbed fibre.

As it will be shown in the following section, mode coupling coefficients m_{ij} can be computed only once for a given z, by numerically solving a modified form of Eq. (2), and amplitudes $A(z)$ and $B(z)$ can be subsequently calculated for every $[A_0, B_0]^T$ without solving a differential equation.

3. Computer-assisted modified coupled-mode method

Equation (2) is a set of two homogenoeus linear first-order ordinary differential equations (ODE) with complex coefficients. With boundary conditions given in the form of

$$\begin{bmatrix} A(0) \\ B(0) \end{bmatrix} = \begin{bmatrix} A_0 \\ B_0 \end{bmatrix} \tag{6}$$

equation (2) forms an initial value problem. Solution of it exists for every $[A_0, B_0]^T$, and it can be expressed as a linear combination of two vector functions $[y_1(z)]$ and $[y_2(z)]$

$$\begin{bmatrix} A(z) \\ B(z) \end{bmatrix} = C_1 \begin{bmatrix} y_{1x}(z) \\ y_{1y}(z) \end{bmatrix} + C_2 \begin{bmatrix} y_{2x}(z) \\ y_{2y}(z) \end{bmatrix} \tag{7}$$

where C_1 and C_2 are complex coefficients, $[y_1(z)]$ and $[y_2(z)]$ are solutions to relation (2) which can be calculated by solving Eq. (2) for two orthogonal boundary conditions $[A_{01}, B_{01}]^T$ and $[A_{02}, B_{02}]^T$.

However, numerical solution of Eq. (2) is time-consuming. In most instances, the moduli of N_{11} and N_{22} are at least three orders of magnitude higher than $|N_{12}|$. As a result Eq. (2) becomes a stiff equation (*cf.* [3]). Moreover, step size Δz has to be lower than 100 nm, in order to achieve acceptable accuracy. From a physical standpoint, the necessity of using such a small value of Δz is easily explainable. Functions $A(z)$ and $B(z)$ describe the amplitude and phase behaviour of electromagnetic field propagating in the fibre. Therefore, to obtain an accurate solution, step size Δz has to be at least one order of magnitude smaller than wavelength λ of the field propagating in the fibre.

Computation time can be substantially reduced if following substitution into Eq. (2) is made:

$$A(z) = C(z)\exp\left(-j\frac{N_{11}+N_{22}}{2}z\right),$$

$$B(z) = D(z)\exp\left(-j\frac{N_{11}+N_{22}}{2}z\right) \tag{8}$$

where $C(z)$ and $D(z)$ are complex functions of z. From the physical standpoint, substitution Eq. (8) can be explained in the following way. In an unperturbed fibre ($N_{11}=N_{22}$ and $N_{21}=0$) propagation constant β equals $(N_{11}+N_{22})/2$. Therefore, the phase of electromagnetic field propagating in the unperturbed fibre is given by the exponential term in Eq. (8), *i.e.*:

$$\exp\left(-j\frac{N_{11}+N_{22}}{2}z\right), \tag{9}$$

and functions $C(z)$ and $D(z)$ are constant and equal A_0 and B_0, respectively. Perturbations acting on the fibre change coupling coefficients N_{ij}. Therefore, the phase of electromagnetic field propagating in the perturbed fibre cannot be expressed only by term (9). As a result, $C(z)$ and $D(z)$, which are no longer constant, contain the correction term which accounts for the phase difference between its actual value in the fibre and our prediction expressed by Eq. (8).

After being rearranged, Eq. (2) becomes

$$\frac{\mathrm{d}}{\mathrm{d}z}\begin{bmatrix} C \\ D \end{bmatrix} = -j\begin{bmatrix} \dfrac{N_{11}-N_{22}}{2} & N_{12} \\ N_{12}^{*} & -\dfrac{N_{11}-N_{22}}{2} \end{bmatrix}\begin{bmatrix} C \\ D \end{bmatrix}. \tag{10}$$

In order to obtain $A(z)$ and $B(z)$ for an arbitrarily chosen $[A_0, B_0]^T$, $C(z)$ and $D(z)$ have to be calculated first. To avoid lengthy recalculation for every A_0, B_0 of interest, Eq. (10) is numerically integrated for two orthogonal boundary conditions: $[0, 1]^T$ and $[1, 0]^T$, yielding two functions $[f_1(z)]$ and $[f_2(z)]$. From linearity of Eq. (10) it follows that for every boundary condition $[A_0, B_0]^T$, which can be written as

$$[A_0, B_0]^T = A_0[1, 0]^T + B_0[0, 1]^T, \tag{11}$$

the solution of Eq. (10) can be expressed as a linear combination of $f_1(z)$ and $f_2(z)$ with identical respective coefficients, *i.e.*:

$$[C(z), D(z)]^T = A_0[f_1(z)] + B_0[f_2(z)]. \tag{12}$$

Therefore, functions $[f_1(z)]$ and $[f_2(z)]$ are calculated only once as $C(z)$ and $D(z)$ can be calculated for every A_0 and B_0, from Eq. (12), by multiplying $[f_1(z)]$ and $[f_2(z)]$ by A_0 and B_0, respectively. Finally, amplitudes $A(z)$ and $B(z)$ are obtained by multiplying $C(z)$ and $D(z)$ by Eq. (9).

It is important to note that most of the time needed to calculate $A(z)$ and $B(z)$ is spent on solving Eq. (10). Subsequent processing, carried out according to Eqs. (12)

and (9), is not time consuming, even if $A(z)$ and $B(z)$ are calculated in a considerable number of points, and for many of boundary condition vectors.

For all weakly guiding fibres the following inequalities hold for $i=1$ and 2:

$$|N_{11} - N_{22}| \ll |N_{ii}|, \tag{13a}$$

$$|N_{12}| \ll |N_{ii}|. \tag{13b}$$

Inequality sign in Eqs. (13a, b) means, for these fibres, a difference of at least two orders of magnitude. By comparing coefficient matrices of Eqs. (2) and (10), one can notice that the off-diagonal elements of both matrices are identical. Moreover, from Eq. (13a) and the accompanying comment, it follows that the absolute values of diagonal elements of the coefficient matrix in Eq. (10) are at least two orders of magnitude smaller that those of diagonal coefficients in Eq. (2). Therefore, when numerical solution of Eq. (10) is performed, step size Δz can be increased at least two orders of magnitude, yielding a hundredfold decrease of computation time.

4. Analysis of a twisted elliptical-core fibre subjected to pure bending

The method introduced in the previous section will be used to calculate visibility at the output of a section of a twisted elliptical-core fibre subjected to pure bending, presented in Fig. 1. Formulae (3)–(5) cannot be applied in such a case because coupling coefficients N_{ij} are functions of fibre axis coordinate z.

Let us assume that light launched into the input of the analysed fibre from a monochromatic source (wavelength $\lambda = 633$ nm) excites both polarization modes with equal amplitudes, and that the phase difference δ between polarization modes can vary

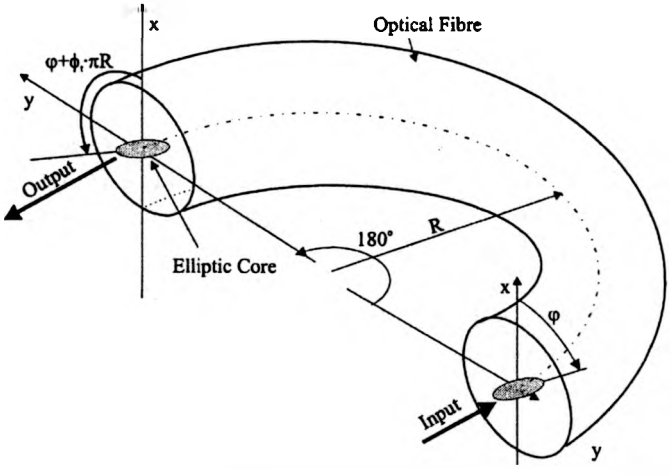

Fig. 1. Section of twisted elliptical-core fibre subjected to pure bending (φ – initial twist angle, ϕ_t – twist rate, R – bend radius).

over an interval greater than 2π radians (such conditions can be encountered, for example, in lead-out fibres of polarimetric optical fibre sensors).

Therefore, the normalized Jones vector describing the state of polarization at the input of the analysed section of the fibre can be expressed as

$$\frac{1}{\sqrt{2}}\begin{bmatrix} 1 \\ \exp(-j\delta) \end{bmatrix} \tag{14}$$

where δ – phase difference between polarization modes. Note that because the axes of the elliptical core do not coincide with x and y axes of the local coordinate system, the components of the Jones vector are amplitudes of polarization modes ${}_oHE_{11}$ and ${}_eHE_{11}$, rather than amplitudes of electric field components E_x and E_y.

Let us also assume that the core of the analysed section of fibre is made of fused silica doped with germanium, while the cladding is made of pure silica. Moreover, it is assumed that both materials are isotropic and follow Hooke's law. Because the values of Young modulus and Poison's ratio of these materials differ by less than 0.1%, the analysed fiber is treated as a homogeneous structure, whose material properties are those of pure fused silica, *i.e.*, Young modulus $E = 7.6\times10^{10}$ N/m^2, bulk modulus $G = 3.27\times10^{10}$ N/m^2 and elastooptic constant $C = 7.6\times10^{-12}$ m^2/N. These assumptions simplified the calculation of the coupling coefficients N_{ij}, which was carried out by following the procedure given in [2], and using analytical expressions derived there and in [1] for the three perturbations of interest.

Finally, let us also assume that the fibre has beat length $l_b = 3$ mm for $\lambda = 633$ nm and that an ideal polarizer is placed at the end of the analysed fibre section, set at 45° to the major axis of the elliptic core of the fibre.

Visibility V is defined as in [4]

$$V = \frac{I_{\max} - I_{\min}}{I_{\max} + I_{\min}} \tag{15}$$

where $I_{\max}$ and $I_{\min}$ are the maximum and minimum intensities. Visibility at the output of the analysed fibre section is a function of bend radius R, twist rate ϕ_t (defined as twist angle per unit length) and initial twist angle φ (defined as the angle between x axis and major axis of elliptic core, *cf.* Fig. 1). All three parameters were varied in order to investigate their effect on visibility. Along with changes of twist rate ϕ_t and initial twist angle φ, the azimuth of the output polarizer was varied, so as to preserve the 45° angle to the major axis of the elliptic core of the fibre. As a result, calculated changes of visibility were caused only by the coupling of polarization modes propagating in the fibre, and not by misalignment of the polarizer.

First, visibility was calculated from formulae (3)–(5) as a function of φ, for the case of no twist (*i.e.*, twist rate $\phi_t = 0$) for different R. This provided reference data for comparison with results obtained using the method presented in Section 3.

Second, two programs were written to perform analysis for $\phi_t \neq 0$. The first program calculates amplitudes $A(z)$ and $B(z)$ by integrating Eq. (2), while the second one uses the modified form Eq. (10) of coupled mode Eq. (2). The output of both programs is visibility V as a function of initial twist angle φ for a given bend radius R and twist rate ϕ_t. Both programs take advantage of linearity of integrated equations, solving them for two sets of boundary conditions, (*cf.* Eqs. (11) and (12)). The fourth order Runge–Kutta method was used in both programs, as it provides good accuracy and short computation time. The integration step was kept constant in order to avoid problems that may sometimes occur with adaptive step-size control algorithms. Moreover, detecting problems caused by numerical instability or by the choice of too long integration step Δz, the total power of electromagnetic field was calculated in every step z_i from relations:

$$P(z_i) = |A(z_i)|^2 + |B(z_i)|^2,$$

$$P(z_i) = |C(z_i)|^2 + |D(z_i)|^2, \tag{16}$$

for the first and second program, respectively. A quality factor η, defined as

$$\eta = \frac{P(z_i) - P(0)}{P(0)}, \tag{17}$$

was subsequently used to compare accuracy of solutions obtained for different step sizes.

Visibility was calculated for twist rate $\phi_t = 0$, $R = 6$, 7 and 10 mm, using both programs and compared with results obtained from Eqs. (3)–(5). Initial twist angle φ was changed from 0° to 180° with a 2°-step. In both cases visibility values agree with each other within 10^{-4}. Subsequently, integration step Δz was adjusted to obtain the same values of quality factor $\eta = 10^{-6}$, and comparison was made of execution times of both programs. The execution times of the first and the second program on a typical desktop PC were about 5400 s and 15 s, respectively. Therefore, the computing time is decreased over two orders of magnitude, as a result of application of the method devised in the previous section, which confirms the prediction expressed therein. The ratio of execution times of both programs remained essentially constant in the calculations described below.

Following successful comparison of results obtained from Eqs. (3)–(5) with those from the program implementing method described in Section 3, visibility was calculated for various twist rates ϕ_t and bend radii R. As the presentation of all results is beyond the scope of the current article and will be the subject of another paper, selected results will be presented to illustrate some of the findings.

In order to determine the influence of low twist rates on visibility, for constant bend radius $R = 7$ mm, calculations were performed for twist rate ϕ_t in the range from 0 to 20 rad/m and initial twist angle φ varied from 0° to 180° with a 2°-step. Since the

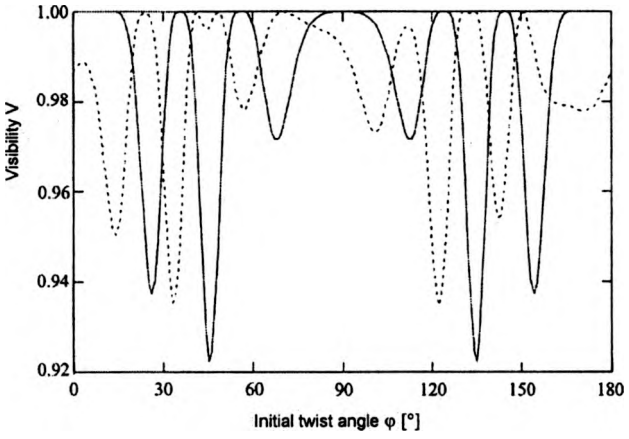

Fig. 2. Visibility as a function of initial twist angle φ (—— twist rate 0 rad/m, - - - twist rate 20 rad/m).

shape of resulting visibility curves does not change much as a function of twist rate ϕ_t, only curves obtained for $\phi_t = 0$ rad/m and $\phi_t = 20$ rad/m are presented in Fig. 2. An interesting feature that can be seen in this figure is an increase of minimal visibility.

To verify whether this phenomenon can be used to improve visibility in bent sections of fibres, calculations were carried out for twist rate ϕ_t in the range from 50 rad/m to 200 rad/m. Calculated visibility curves for 20 rad/m, 50 rad/m and 100 rad/m are shown in Fig. 3. Interestingly, minimum visibility increases from 0.922 for no twist, up to 0.971 for twist rate of 50 rad/m, and then decreases again, falling to 0.959 for twist rate of 200 rad/m. Moreover, as can be seen in Fig. 3, the shape of visibility curves for twist rates higher than 20 rad/m loses its regularity clearly visible for visibility curves obtained for lower twist rates (*i.e.*, $\phi_t = 0$ rad/m and $\phi_t = 20$ rad/m) shown in Fig. 2.

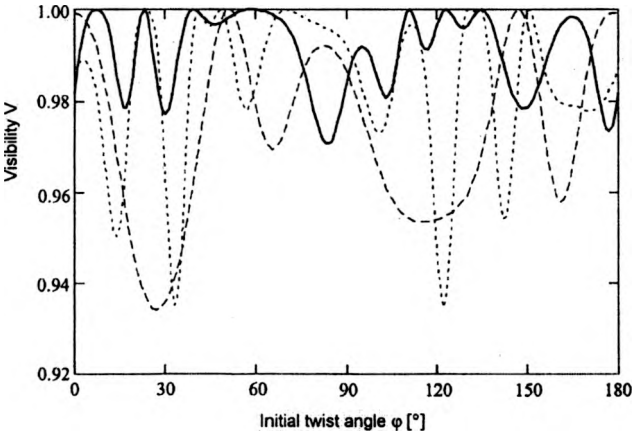

Fig. 3. Visibility as a function of initial twist angle φ (· · · · twist rate 20 rad/m, —— twist rate 50 rad/m, - - - twist rate 100 rad/m).

Even though the increase of minimum visibility is clearly visible, it is far-fetched to claim that the visibility can be improved by introducing controlled twist in the bent fibre. One should remember that some twist may exist in the fibre as a result of drawing process, which, adding to the controlled twist, may greatly decrease visibility instead of increasing it.

5. Conclusions

Presented in the paper computer-assisted modified coupled-mode method is a versatile tool for calculating the evolution of the SOP along a single-mode fibre subjected to multiple perturbations. Contrary to other approaches the method can be applied when coupling coefficients N_{ij} are functions of location z along the fibre.

Example of calculations illustrates the use of the method for design of a polarimetric optical fibre sensor. The present method does not restrict the length of analysed fibre section which can reach several meters. Moreover, speed at which calculations are performed can be increased by using another, more effective ODE solver featuring also adaptive step-size control.

The method can be further extended to provide results not only for the case of a strictly monochromatic source, but also for sources such as light emitting diodes (LEDs) or superluminecent diodes (SLDs).

References

[1] JUN-ICHI SAKAI, TATSUYA KIMURA, IEEE J. Quantum Electron. **17** (1981), 1041.

[2] JUN-ICHI SAKAI, TATSUYA KIMURA, IEEE J. Quantum Electron. **18** (1982), 59.

[3] PRESS W.H., FLANNERY B.P., TENKOLSKY S.A., VETTERLYNG W.T., *Numerical Recipes in C – The Art of Scientific Computing*, Cambridge University Press, Cambridge, New York 1992.

[4] BORN M., WOLF E., *Principles of Optics*; Pergamon Press, London 1996 (Sixth edition).

Received October 17, 2001